The Astrophysical Journal, 604:455–468, 2004 March 20

LOOKING FOR GRAVITY-MODE MULTIPLETS WITH THE GOLF EXPERIMENT ABOARD *SOHO*

S. Turck-Chièze,[1] R. A. García,[1] S. Couvidat,[1,2] R. K. Ulrich,[3] L. Bertello,[3] F. Varadi,[3] A. G. Kosovichev,[2] A. H. Gabriel,[4] G. Berthomieu,[5] A. S. Brun,[1] I. Lopes,[6,7] P. Pallé,[8] J. Provost,[5] J. M. Robillot,[9] and T. Roca Cortés[8]

Received 2002 April 26; accepted 2003 December 2

ABSTRACT

This paper is focused on the search for low-amplitude solar gravity modes between 150 and 400 μHz, corresponding to low-degree, low-order modes. It presents results based on an original strategy that looks for multiplets instead of single peaks, taking into consideration our knowledge of the solar interior from acoustic modes. Five years of quasi-continuous measurements collected with the helioseismic GOLF experiment aboard the *SOHO* spacecraft are analyzed. We use different power spectrum estimators and calculate confidence levels for the most significant peaks. This approach allows us to look for signals with velocities down to 2 mm s^{-1}, not far from the limit of existing instruments aboard *SOHO*, amplitudes that have never been investigated up to now. We apply the method to series of 1290 days, beginning in 1996 April, near the solar cycle minimum. An automatic detection algorithm lists those peaks and multiplets that have a probability of more than 90% of not being pure noise. The detected patterns are then followed in time, considering also series of 1768 and 2034 days, partly covering the solar cycle maximum. In the analyzed frequency range, the probability of detection of the multiplets does not increase with time as for very long lifetime modes. This is partly due to the observational conditions after 1998 October and the degradation of these observational conditions near the solar maximum, since these modes have a "mixed" character and probably behave as acoustic modes. Several structures retain our attention because of the presence of persistent peaks along the whole time span. These features may support the idea of an increase of the rotation in the inner core. There are good arguments for thinking that complementary observations up to the solar activity minimum in 2007 will be decisive for drawing conclusions on the presence or absence of gravity modes detected aboard the *SOHO* satellite.

Subject headings: Sun: helioseismology — Sun: interior — Sun: oscillations

On-line material: color figures

1. INTRODUCTION

Helioseismology has demonstrated its ability to probe the solar interior. The *Solar and Heliospheric Observatory* (*SOHO*) mission, launched on 1995 December 2, offers a unique opportunity for studying the Sun because of the exceptional properties of the spacecraft. It is above any atmospheric perturbations, at the Sun-Earth Lagrangian point L1, and has an expected lifetime of about a solar cycle (11 yr). Three experiments dedicated to helioseismology have been placed on board: Global Oscillations at Low Frequencies (GOLF; Gabriel et al. 1995), Solar Oscillations Investigation/Michelson Doppler Imager (SOI/MDI; Scherrer et al. 1995), and Variability of Solar Irradiance and Gravity Oscillations (VIRGO; Fröhlich et al. 1995). Intercomparison between them (Toutain et al. 1997) has showed the importance of properly understanding acoustic-mode excitation and the asymmetric profiles that depend on the nature of the measurements (Nigam & Kosovichev 1999; Thiery et al. 2000, 2001; Basu, Turck-Chièze, & Berthomieu 2000; Bertello et al. 2000a).

At the current state of the art, this discipline puts strong constraints on the microscopic physics introduced in stellar evolution models of solar-like stars on the main sequence, probing the ionization degree of individual species, relativistic effects, bound-bound processes, and nuclear interactions (Vorontsov, Baturin, & Pamyatnykh 1991; Turck-Chièze et al. 1997, 1998b; Elliott & Kosovichev 1998; Turck-Chièze et al. 2001a, 2001b). The simultaneous determination of the rotation and the sound speed profiles is crucial for modeling macroscopic motions present in the outer layers, in the convective zone, and at its base (Kosovichev et al. 1997; Corbard et al. 1998). These studies lead to the introduction of new terms in the stellar structure equations that were previously ignored, such as mixing induced by turbulent diffusion, rotation, and magnetic field (Elliott & Gough 1999; Brun, Turck-Chièze, & Zahn 1999; Maeder & Meynet 2000; Demarque & Robinson 2003). Nowadays the sound speed and the density are determined down to about 0.07 $R_\odot$ with an accuracy of better than 10^{-3}, thanks to the detection of the low-order acoustic modes (Bertello et al. 2000b; García et al. 2001a). These modes are much less sensitive to the surface layers than those with higher frequencies. In particular, the temporal dependence of the outer layers due to the solar cycle can be practically avoided and the frequency determination improved because of a reduced influence of the stochastic excitation. These modes have allowed the rejection of some phenomena as important for mixing in

[1] CEA/DSM/DAPNIA, CE Saclay, 91191 Gif sur Yvette, France; cturck@cea.fr.
[2] W. W. Hansen Experimental Physics Laboratory, Stanford University, Stanford, CA 94305-4085.
[3] Department of Physics and Astronomy, University of California, Los Angeles, CA 90095-1562.
[4] Institut d'Astrophysique Spatiale, Orsay, France.
[5] Observatoire de la Côte d'Azur, Laboratoire Cassini CNRS URA1362, 06304 Nice, France.
[6] Department of Physics, Nuclear and Astrophysics Laboratory, Keble Road, Oxford OX1 3RH, UK.
[7] Instituto Superior Técnico, Avenida Rovisco Pais, Centro Multidisciplinar de Astrofísica, 1049-001 Lisbon, Portugal.
[8] Instituto de Astrofísica de Canarias, E-38205 La Laguna, Tenerife, Spain.
[9] Observatoire de l'Université Bordeaux 1, BP 89, 33270 Floirac, France.

the core and strong dynamical screening that were invoked in the past (Turck-Chièze et al. 2001a). From these modes, we build seismic models from which we deduce the neutrino flux emissions (Takata & Shibahashi 1998: Turck-Chièze et al. 2001b; Couvidat, Turck-Chièze, & Kosovichev 2003b). But these low-frequency p-modes are not sensitive enough to the very central region of the Sun. As a consequence, the spatial resolution reached in the nuclear core is only $\pm 3\%$ (Turck-Chièze et al. 2001a, 2001b). Furthermore, because of the inherent p-mode characteristics, the accuracy and the spatial resolution in the core are not sufficient to extract the inner dynamics. The rotation of the very inner region is presently not accessible. The current estimates of a rigid-body rotation in the radiative region down to 0.15 $R_\odot$ (Corbard et al. 1999; Couvidat et al. 2003a) show that the uncertainties are still large when going deeper in the core, and the improvement of the present situation supposes the detection of at least some mixed modes at lower frequencies.

All these reasons encourage the search for another class of solar oscillations, called gravity modes, that are trapped in the radiative zone and largely influenced by the physics of the nuclear region. In fact, 75% of the gravity-mode inertia comes from the region below 0.2 $R_\odot$. Figure 1*a* shows the propagation region for an acoustic mode of degree $l = 1$ and frequency $\nu = 1500$ μHz (Lopes & Turck-Chièze 1994), and Figure 1*b* shows the potential corresponding to a gravity mode of degree $l = 2$ and radial order $n = -3$. This representation is obtained by an procedure analogous to the one developed for the acoustic modes by Lopes & Gough (2001 and references therein). The motion equation for the solar gravity oscillations is approximated by $\ddot{\Psi} + \kappa_r^2 \Psi = 0$, where Ψ is the radial component of a wave function proportional to the Lagrangian perturbation of pressure, κ_r is the vertical component of the wavenumber, and a dot denotes differentiation with respect to the independent variable. In that case, κ_r^2 is approximated by $l(l+1)/(2\pi P)^2 \mathrm{sgn}(N^2) - \mathcal{G}^2$, where P is the period of the gravity wave, $\mathcal{G}^2$ is the gravity potential, and $\mathrm{sgn}(N^2)$ gives the sign of the squared Brünt-Väisälä frequency. The gray rectangle on the right defines the region of the star where $\mathrm{sgn}(N^2)$ is equal to -1 (i.e., mainly the convective region). As usual, the mode propagates in the region where $\kappa_r > 0$ and is evanescent elsewhere. One notices that the low-degree, low-order modes are very sensitive to the base of the convective region and to the central region of the Sun, i.e., at the location of the inner and outer turning points.

The determination of the gravity-mode characteristics is crucial for understanding the density and the mass distribution. Their sensitivity to any physical process is about 10 times greater than the sensitivity of the global acoustic modes (Brun, Turck-Chièze, & Morel 1998; Provost, Berthomieu, & Morel 2000, hereafter PBM00). Furthermore, it has been proposed that the very low frequency gravity-propagating waves would be extremely important in redistributing angular momentum inside the radiative zone (Kumar, Quataert, & Eliot 1997; Zahn, Talon, & Matias 1997; Kumar, Talon, & Zahn 1999). It may also look for the existence of local instabilities in the core and some manifestation of the central magnetic field.

In the present paper the strategy followed to search for gravity modes is presented in § 2. In § 3 we describe the methods to produce the different power spectra used in this work, and in § 4 we describe the statistical approach. In § 5 we present the results for the first 1290 days of GOLF observations, mainly corresponding to a quiet Sun, and the detection of promising peaks or multiplets with a 90% confidence level of not being pure noise. In § 6 we discuss how the structures evolve over 1768 and 2034 days. Finally, we comment in the last two sections on the possible identification of the residual candidates and on future work.

2. THE STRATEGY USED FOR THE GRAVITY-MODE SEARCH

Gravity modes have not been unambiguously detected after 20 years of effort with ground-based networks, although several attempts have been made (e.g., Delache & Scherrer 1983; van der Raay 1988; Martín Mateos & Pallé 1999), nor from space (Thomson, Maclennan, & Lanzerotti 1995), where authors have claimed to detect gravity modes below 140 μHz but recent studies have not confirmed these claims (e.g., Denison & Walden 1999). In the past, most of the search was based on the asymptotic properties of the g-modes (e.g., Fröhlich & Delache

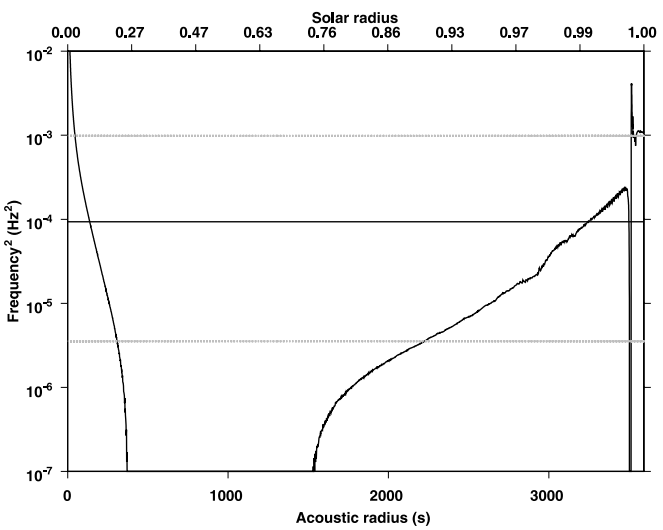

FIG. 1*a*

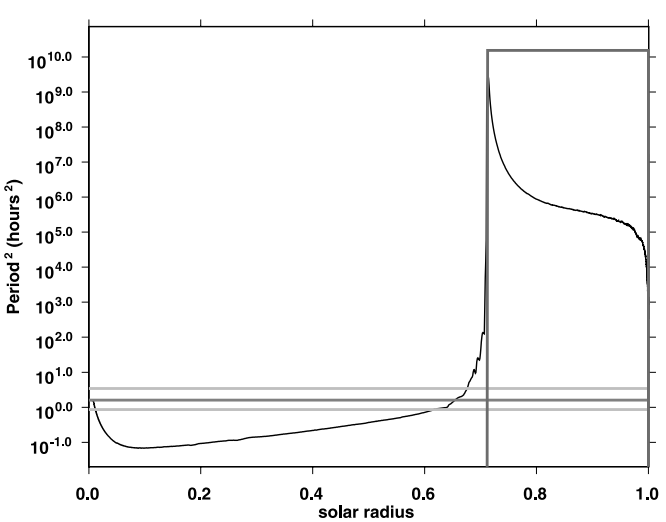

FIG. 1*b*

FIG. 1.—(*a*) Variation of the square of the acoustic potential with acoustic radius and solar radius for $l = 1$ and $\nu = 1500$ μHz. The frequency of the mode is represented by a black line, and the gray dotted lines correspond to modes of 5000 and 300 μHz (Lopes & Turck-Chièze 1994; Lopes & Gough 2001). (*b*) Variation of the square of the gravity potential with the Sun's radius. This potential is computed for $l = 2$, $n = -3$ ($P = 1.26$ hr). The period of this mode is represented by the black line. The light gray lines define the observational window for gravity-mode detection: 150–400 μHz.

1984; Pallé et al. 1998). Unfortunately, this type of analysis concerns modes of low-degree but high-order that have low frequencies ($\nu < 100$ μHz). The search is extremely difficult in this frequency range because the gravity modes are probably damped in the radiative region by the μ-gradient of the composition in the nuclear core. This radiative damping has been estimated by Zahn et al. (1997) and has a frequency dependence of $[l(l+1)]^{3/2}/\omega^4$. This frequency dependence probably explains why such modes have not been detected yet. Even with *SOHO* this range seems today inaccessible. Thus, our search has been oriented toward the upper region of the gravity spectrum (Kosovichev & Gavryuseva 1995) and finding multiplets to reduce the detection limit (Turck-Chièze et al. 1998a). It has led to the discussion of two candidates centered around 220.6 and 251.8 μHz mentioned in Gabriel et al. (1998). For the single peaks, the limit of 1 cm s^{-1} has been obtained by the Phoebus group (Appourchaux et al. 2000) after 2 years of observations with MDI and VIRGO and the long-term ground-based BiSON network data. A new limit of 6 mm s^{-1} has recently been discussed using the GOLF instrument after 5 years of observations (Gabriel et al. 2002). The difficulty of detecting gravity modes is twofold:

1. They are in the 10–400 μHz frequency range, where the power spectrum is dominated by the incoherent superficial motions of the Sun (mainly granulation).
2. Their surface amplitudes are predicted to be extremely small because of their evanescent character in the convective region. Thus, only those gravity oscillations of lower degree are expected to have vertical components large enough to be detected. Of course, their energy depends on the excitation mechanism, which is not totally understood, and their predicted surface amplitudes vary from 0.01 up to a few mm s^{-1}, depending on the frequency and on the hypotheses introduced in the calculations (Andersen 1994, 1996; Kumar, Quataert, & Bahcall 1996; PBM00).

To improve the *g*-mode search, one needs to reduce the detection amplitude threshold while keeping a high confidence level. Thus, we have defined the following strategy:

1. *To look for g-modes with frequencies above* 150 μHz.—In this range, the corresponding *g*-modes are probably as excited by the turbulent convection as the *p*-modes are. In this case, the radiative damping rate varies as the square of the mode order *n*, whereas the turbulent damping rate is a weak function of *n* (Kumar et al. 1996). So, the surface velocity amplitude is almost independent of *l* and larger for low-order modes, with a decrease of nearly a factor of 10 between 200 and 100 μHz. A calculation of the inertia of these modes confirms this expectation (PBM00).
2. *To look for g-mode–like structures in an interval of* ± 10 μHz *around the corresponding theoretical frequency.*—This large interval of 20 μHz is very conservative and provides enough room for a frequency shift due to unexpected variations of the very inner core. In fact, different studies have shown that the sensitivity to classical physical processes inside the radiative zone or in the upper layers is less than 5 μHz (Brun et al. 1998; PBM00). In this paper we use as predicted *g*-modes the theoretical estimates deduced from our seismic model (Turck-Chièze et al. 2001b). This model has been computed to reproduce the observed squared solar sound speed in the core. As we are interested in multiplets, centering the search of mode in the window assures that the full multiplet is inside our box, preventing the use of a systematic scan between 150 and 400 μHz.
3. *To look for singlets and multiplets*.—Assuming that GOLF can observe only those components for which $l + m$ is an even number, we look for singlets, doublets, and triplets. However, it is not excluded that some components will not be visible at a given time because of, e.g., the interference of noise, already observed in the *p*-mode range. To define the multiplets, we have limited the rotational splitting between two adjacent components to 0.2 $\mu\text{Hz} < \delta\nu < 0.6$ μHz (following PBM00). This range allows the possibility of an increase or a reduction of the rotation profile in the solar core. We have also assumed an equidistance (symmetry) between the components of the multiplet within 0.15 μHz. Therefore, even if the probability of each individual component of a multiplet containing signal is small, the probability for the whole multiplet is higher, as is shown by Monte Carlo simulations in § 4. In fact, this third criterion is extremely strong in reducing the detection threshold while keeping the same confidence level. However, it assumes only small asymmetries due to effects such as the magnetic field, which is justified by our knowledge of acoustic modes. This point could be readjusted in the future if necessary.
4. *To estimate the confidence levels of the structures observed in different power spectrum estimators*.—These include periodograms with zero-padding and averaged–cross spectrum (AvCS) and multitaper (MT) analyses (see Appendices A–D). We discuss in this paper the cases where the confidence level of finding singlets, doublets, triplets, or a larger number of components that are not purely noise exceeds 90%. This criterion greatly reduces the range of examined amplitudes. We then use the theoretical frequency values, constrained by acoustic modes, to propose a possible identification of the candidates.
5. *To follow the temporal evolution of the detected structures*.—The main analysis is done with 1290 days recorded mostly during the solar minimum. Two longer series were considered with lengths of 1768 and 2034 days.

Once we have defined our strategy to search for gravity modes, we have to determine the time series to be used, as well as the best power spectrum estimators.

3. METHODS USED TO ANALYZE THE GOLF DATA

The GOLF experiment measures the integrated line-of-sight velocity between the Sun and the spacecraft from two spectroscopic observations of one wing of the sodium doublet separated by ~77 G (Gabriel et al. 1995, 1997; Ulrich et al. 2000a). These measurements are recovered every 10 s by two independent photomultipliers and have been resampled to 80 s for the present work. The calibration procedure for extracting the velocity from the original one-wing observation is based on the methods described in Ulrich et al. (2000b) for the random-lag singular cross spectrum analysis (RLSCSA) and García, Turck-Chièze, & Boumier (2003) for the other analyses. In both calibration methods we correct all the fluctuations of the detectors and consequently use the complete statistics accumulated on the two photomultipliers. Since we are interested only in frequencies above 150 μHz, we have applied a digital high-pass filter with a 11.57 μHz cut-on frequency. The measurements started on 1996 April 11 on the left side (blue wing) of the sodium lines, up to the loss of *SOHO* on 1998 June 25. After the recovery of the instrument, GOLF was restarted on the right side (red wing) of the sodium lines. The impact of such a change is not easy to estimate for the search for *g*-modes, but it is now well established for *p*-modes that it is not the best way to observe low-amplitude signals. This

is the reason why GOLF was switched back to the blue wing configuration on 2002 November 18.

In this paper we start by analyzing a time series of 1290 days. This one contains the previously analyzed 805 days on the blue wing (reported in Gabriel et al. 1998). It has a global duty cycle of better than 88% from 1996 April 11 to 1999 October 22. This rather small value of the duty cycle is due to the temporary loss of *SOHO*. The effective duty cycle of normal GOLF operations is more than 99%. This series stops before the solar maximum. Then two other analyses are done, after 1768 and 2034 days, covering the solar maximum.

Other analyses have also been done, in particular, dividing the complete series into two parts, before (blue wing) and after (red wing) the *SOHO* vacations, but the conclusions we obtain in this paper are not affected.

3.1. *Power Spectrum Estimators*

The standard way to extract frequencies of coherent periodic signal from a noisy background is to compute the fast Fourier transform (FFT) of the time series. If the mode is not resolved (longer lifetime than the duration of observations) or if it is not re-excited, then the peak in the periodogram estimator will be a squared cardinal sine (because of the finite observational window) centered at the frequency of the mode. However, if this frequency is not an integer number of the discrete FFT frequency sampling, the power of the mode will not be concentrated in one bin but spread between two adjacent bins. In the worst case, the reduction in the power amplitude could be 40%, and an analysis based on the search of peaks above a certain level could fail to detect it. In our case, we use a periodogram with zero-padding by a factor of 3, which reduces this effect to 9%. As explained in Gabriel et al. (2002), with zero-padding by a factor of 5 we can even decrease this effect to less than 3%.

To avoid any bias coming from the chosen power spectrum estimator, we have decided to use other methods that have been developed recently, the AvCS, the MT indicator (Komm et al. 1998), which is also less sensitive to the previous problem (<10%), and the RLSCSA (Varadi et al. 2000). A detailed description of the power spectrum density (PSD) estimators is presented in Appendices A–D.

Since the gravity-mode search is a difficult task, we discuss in the following the zero-padded FFT and the MT analyses for which we have calculated confidence levels. The results obtained with the AvCS do not change the conclusions of the paper; this estimator reduces in interest as the length of the series increases. The statistical analysis of the RLSCSA spectra turns out to be more difficult than that for the other methods (Couvidat 2003). It is not easy to find by a mathematical approach the statistical distribution of noise in this analysis. Moreover, the ability of this method to produce very high noise peaks makes it inappropriate to apply our statistical approach to it. However, it is important to remember that the first low-degree, low-order *p*-modes below 1 mHz were detected using this method before being confirmed by other techniques (Bertello et al. 2000b). Such analysis has shown interesting features for some candidates, as discussed below.

Since we study the upper frequency range of the gravity modes where the amplitudes are expected to be the highest, the excitation of these modes is located in the upper layers of the convective zone and could be damped on timescales comparable to the duration of observations. Thus, because of their mixed character, we cannot exclude possible re-excitations of these modes. To check the impact of this effect on the spectrum estimators, we introduce a phase shift in a sinusoidal wave. We have noticed that such a change spreads the power between the adjacent bins on the periodogram. This spread is important to quantify since our search is based on peaks above a given threshold. The amount of this power leakage will depend on the position and on the value of the phase shift. Analytically, it can be demonstrated that in the worst case, with a phase shift of 180° just in the middle of the series, the power will be reduced by nearly 50% in the periodogram. With a periodogram with zero-padding by a factor of 3, the reduction is $\sim$30%, while for the MT analysis (four tapers), it is less than 3% (García et al. 2001b). This behavior gives strong support to the MT analysis in our search.

3.2. *Treatment of the Solar Background Noise*

In the spectral region of interest (150–400 μHz), the instrumental noise is nearly 1 order of magnitude lower than the solar noise (see Fig. 2). This is due to the stability and performance of the GOLF instrument (Gabriel et al. 1995, 1997; Dzitko 1995). Therefore, the power spectrum estimate at this frequency range is dominated by the convective random motions, mainly the granulation contribution. To take it into account, a two-component fitting (granulation and supergranulation) following the model of Harvey (1985) was done between 50 and 1200 μHz. The estimator was normalized by the resultant fitting, and a flat spectrum was obtained. Hereafter, the MT and the zero-padded periodogram were divided by the fitted background. Furthermore, every individual 20 μHz region was renormalized by its local noise standard deviation. In the case of the RLSCSA analysis, the spectrum was pre-whitened using methods described by Percival & Walden (1993).

4. THE STATISTICAL ANALYSIS

We search for *g*-modes on the GOLF power spectra in frequency intervals of width $\Delta_{\rm det}$ μHz. Suppose we detect a structure—a peak or a group of peaks—that might be a gravity mode. We need to resort to a statistical analysis to answer the question, what is the probability $p_{\rm signal}$ that this structure detected in $\Delta_{\rm det}$ does contain signal (i.e., is not pure noise)? This question is closely related to the question, what is the probability that this structure has been produced by noise only, i.e., what is the probability that noise produces such a structure, i.e., what is the probability $p_{\rm noise}$ that such a structure is present in any $\Delta_{\rm det}$ interval on the power spectrum of a Gaussian noise series? The relation between the two probabilities is $p_{\rm signal} = 1 - p_{\rm noise}$. The computation of $p_{\rm noise}$ requires knowing the statistical distribution of noise on the power spectra and then (analytically or numerically) deriving the probabilities $p_{\rm noise}$ for each type of structure that we are looking for and for each type of spectrum. Actually, to derive relevant $p_{\rm noise}$ probabilities, we add information to the statistical analysis: the detected structure is compatible with a $l = 2$ doublet (for instance). However, that does not mean that we assume that the structure we observe is a $l = 2$ doublet (such a statement would mean an a priori assumption that the structure contains signal). The term $p_{\rm noise}$ depends on the type of structure that we are interested in: the probability that pure noise produces a structure compatible with an $l = 2$ doublet is different from the probability that pure noise produces a structure compatible with an $l = 3$ triplet. It is important to note that the statistical analysis is in no way intended to help us in identifying the *g*-mode candidate. We only mention that the detected

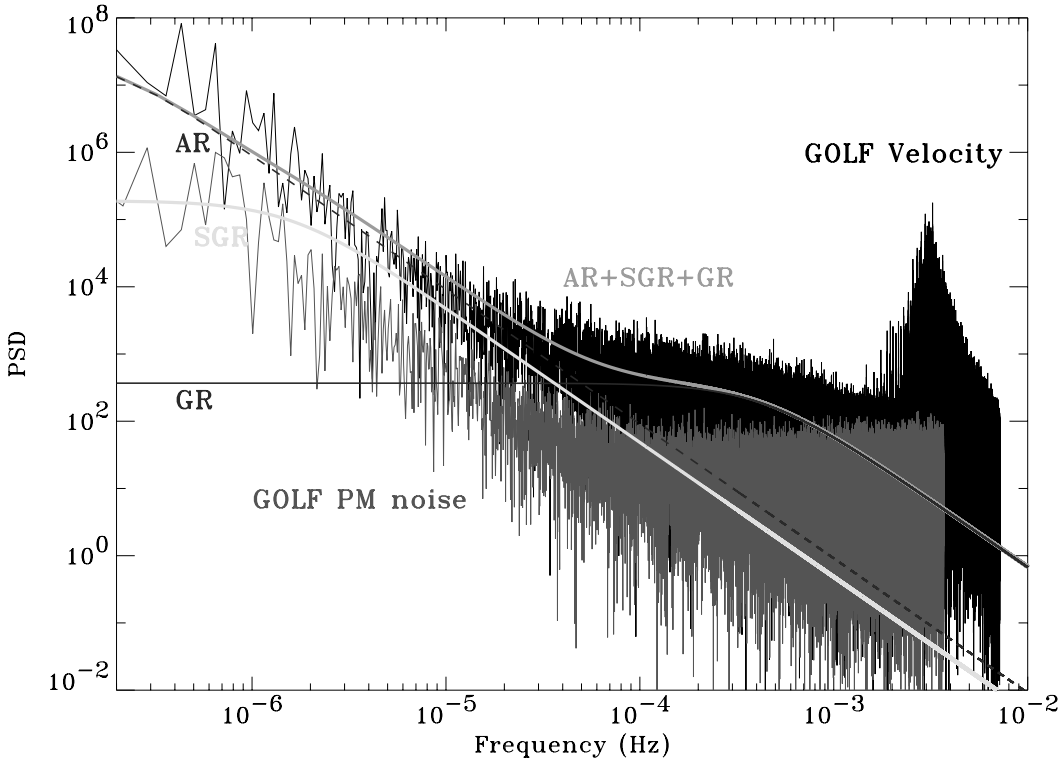

FIG. 2.—PSD of the GOLF spectrum in black. The gray spectrum corresponds to the GOLF instrumental noise. Between 150 and 400 μHz the level of photon noise is about 1 order of magnitude lower than the velocity continuum. The continuous lines are the fitted Harvey model for the active regions (ARs), granulation (GR), supergranulation (SGR), and the sum of all three (AR + SGR + GR). The continuum is dominated by the granulation in the region of interest. [*See the electronic edition of the Journal for a color version of this figure.*]

structure is compatible with an $l = 2$ doublet, and then we derive the probability $p_{\rm noise}$ that pure noise produces two peaks compatible with an $l = 2$ doublet in a $\Delta_{\rm det}$ interval.

4.1. *The Approach Used*

The structures that we try to detect are the singlets, the $l = 1,\ 2,\ 3$ doublets, and the $l = 2,\ 3$ triplets. A singlet is a single peak whose amplitude is larger than a given threshold $S_{\rm det}$ (see previous searches, Appourchaux et al. 2000; Gabriel et al. 2002). A doublet is a structure of two peaks whose amplitudes are larger than $S_{\rm det}$ and with a separation between these two peaks lying within a given range. This range is 0.4–1.2 μHz for an $l = 1$ doublet (we can detect only the $m = -1$ and $m = +1$ components with GOLF), 0.4–2.4 μHz for an $l = 2$ doublet (in the worst case we detect $m = -2$ and $m = +2$), and 0.4–3.6 μHz for $l = 3$. An $l = 2$ triplet is a structure of three peaks whose amplitudes are larger than $S_{\rm det}$, with a separation between the three peaks lying within a given range, and with a symmetry requirement (the difference between the two separations must be ≤ 0.15 μHz). For the $l = 3$ triplets three configurations are to be considered, depending on the component visibility: $m = -3,\ -1,\ +1$ or $m = -1,\ +1,\ +3$, $m = -3,\ +1,\ +3$, and $m = -3,\ -1,\ +3$. It is noticeable that, for instance, an $l = 1$ doublet is compatible with an $l = 2$ doublet. What $p_{\rm noise}$ probability is relevant in this case? If the solar models predict no $l = 1$ mode but one $l = 2$ mode in the given $\Delta_{\rm det}$ interval and we have detected a structure of two peaks, we compute $p_{\rm noise}$ related to the case "structure compatible with an $l = 2$ doublet." If the solar models predict the presence of both $l = 1$ and $l = 2$ modes, and the observed structure is compatible with both of them, we can either apply the most restrictive case (we compute $p_{\rm noise}$ related only to the $l = 1$ doublet) or give $p_{\rm noise}$ probabilities for the $l = 1$ and $l = 2$ doublets.

On a time series (i.e., a series of solar surface velocity as a function of time), the solar noise follows a Gaussian distribution. On a periodogram of such a series, the statistical fluctuation of solar noise is distributed as a scaled χ^2 with 2 degrees of freedom (χ^2_2). On the AvCS and MT power spectra, the probability distribution is a χ^2 with $2N$ degrees of freedom (χ^2_{2N}). N is the number of averaged series for the AvCS and the number of tapers for the MT. The easiest $p_{\rm noise}$ to derive is the probability that any given $\Delta_{\rm det}$ interval on the periodogram of a Gaussian noise series contains a singlet: $p_{\rm noise} = 1 - (1 - p)^{N_p}$ (Appourchaux et al. 2000). N_p is the number of peaks in $\Delta_{\rm det}$, and p is the probability of a given noise peak exceeding $S_{\rm det}$: $p = \exp(-S_{\rm det})$ for a χ^2_2 distribution if $S_{\rm det}$ is in units of the noise standard deviation σ; $p_{\rm noise}$ depends on the width of the $\Delta_{\rm det}$ interval: the larger that $\Delta_{\rm det}$ is, the more likely the presence of a noise singlet is. For the g-mode search we choose $\Delta_{\rm det} = 20$ μHz.

The previous analytical approach cannot be applied to the derivation of other $p_{\rm noise}$ related to a singlet on the AvCS and the MT because the frequency bins are correlated with these power spectrum estimates. For $p_{\rm noise}$ related to doublets and triplets, we also resort to Monte Carlo simulations: we produce Gaussian noise series, we compute their periodogram, their zero-padded periodogram, their AvCS, and their MT, and then we apply our detection algorithm on these spectra. This algorithm searches for singlets, doublets, and triplets. The parameters of the search are the length T of the time series (in days), $\Delta_{\rm det}$ (in μHz), $S_{\rm det}$ (in σ units), the different separations

TABLE 1
DETECTION THRESHOLD S_{DET} (IN σ) AND CORRESPONDING PROBABILITIES (IN PERCENT) OF FINDING NOISE PEAK FOR THE TWO POWER SPECTRUM INDICATORS

		DOUBLET			TRIPLET	
THRESHOLD	SINGLE PEAK	$l = 1$	$l = 2$	$l = 3$	$l = 2$	$l = 3$
Periodogram with Zero-padding						
11.1.....	10.08	0.03	0.09	0.15	0.00	0.00
8.1.....	83.11	10.07	20.69	27.89	0.25	1.23
8.5.....	66.71	4.46	10.01	14.08	0.06	0.32
8.8.....	61.00	3.14	6.88	10.00	0.03	0.18
6.7.....	99.82	66.27	86.30	92.10	10.01	31.18
7.3.....	97.85	36.62	59.25	69.68	2.52	10.05
Multitaper						
8.0.....	10.03	0.03	0.09	0.17	0.00	0.00
6.2.....	82.66	10.04	20.13	27.14	0.29	1.20
6.5.....	68.93	4.72	10.00	14.36	0.08	0.35
6.6.....	61.20	3.15	6.92	10.00	0.03	0.16
5.4.....	99.81	66.21	85.76	91.62	10.00	30.30
5.7.....	97.93	36.68	58.55	68.80	2.53	10.00

that we allow between the components of the multiplets, and the asymmetry of the two separations of the triplets. We base our estimation of each p_{noise} on at least 50,000 realizations.

To make clear the meaning of the probabilities that we obtain with these Monte Carlo simulations, we consider for example the $l = 2$ doublet: suppose we want to know the probability that two peaks compatible with an $l = 2$ doublet in a Δ_{det} interval on an MT of length T are due only to noise. We produce 50,000 different Gaussian noise series of length T. We compute their MT. We divide each MT into N_{int} frequency intervals of width Δ_{det} μHz. In each interval the detection algorithm searches for a structure compatible with an $l = 2$ doublet (i.e., a structure following the definition previously given). The algorithm selects the peaks larger than S_{det} and then checks if there exists any combination of two selected peaks with a separation within the allowed range. Eventually, after 50,000 realizations, the number of intervals in which at least one such structure has been found is divided by the total number of intervals ($N_{int} \times 50{,}000$). Thus we obtain the probability that noise produces a structure compatible with an $l = 2$ doublet in a frequency interval Δ_{det} on an MT of length T. If the study of a frequency interval on a GOLF MT reveals a structure compatible with an $l = 2$ doublet, we know the related probability p_{noise} of this structure to have been produced by noise only, and thus its probability $p_{signal} = 1 - p_{noise}$ of containing signal. Table 1 summarizes the values of p_{noise} for the different structures we are looking for with the zero-padded periodogram and MT. We give these probabilities as a function of S_{det}. The probabilities related to noise doublets are rather small, and the probabilities that noise produces an $l = 2$ or $l = 3$ triplet are extremely low. We note for example that for the zero-padded periodogram, the probability to have a noise peak with an amplitude larger than 8.55 σ is 66.71% in an interval of 20 μHz. This probability is only 10% for the doublets $l = 2$. That means that each doublet compatible with a mode $l = 2$ and with an amplitude larger than 8.55 σ has a probability of 90% of containing signal. This confirms the interest in our method of detecting modes whose individual components have low amplitudes: we compensate these low amplitudes by detecting several components. To detect g-mode candidates, we have used the Monte Carlo simulations to derive the different thresholds for which the corresponding p_{noise} is less than 0.1. We call this analysis the "better than 90% confidence level criterion." Thus, if we detect a structure compatible with an $l = 2$ doublet with its two components above the threshold corresponding to the "better than 90% confidence level criterion" for $l = 2$ doublets, we know that this possible g-mode has a probability of at least 90% of containing signal. We call detection thresholds the S_{det} values corresponding to $p_{noise} = 0.1$ for the different structures. Figure 3 shows an example of p_{noise} values for the different singlet and multiplets we have defined, as a function of the S_{det} values for an MT of length $T = 1290$ days. On this figure, the horizontal line corresponds to $p_{noise} = 0.1$. For a given S_{det} value, p_{noise} for an $l = 3$ triplet is higher than for an $l = 2$ triplet, because there are three different configurations compatible with an $l = 3$ triplet (we have to pick three peaks out of the four visible by GOLF) and only one compatible with an $l = 2$ triplet: it is "easier" to produce a structure similar to an $l = 3$ triplet.

To conclude this section, it is also noticeable that if a structure appears in at least two different PSD estimates (MT and periodogram, for instance), it has a better chance of containing signal, even if the data used to compute the spectra are the same. This point has also been demonstrated by Monte Carlo simulations. We produce random time series and apply our three PSD estimates to each of them. We conclude that a noise peak above the threshold defined by a given p_{noise} in a periodogram has only a 9.5%–13.5% chance (for respectively $p_{noise} = 0.1$–0.9) of appearing in the same condition in the MT analysis. The probability of a noise peak reaching the corresponding threshold in the three spectra is smaller: less than 8% for $p_{noise} \leq 0.9$. As mentioned in § 5, some of our g-mode candidates appear in two or three different analyses, encouraging the belief that they are not purely due to noise.

4.2. *Verification of the Statistical Assumption Made on Real Data*

We have checked the assumptions of our statistical analysis on GOLF spectra. First, the GOLF time series follow a Gaussian distribution to a very good approximation, whatever

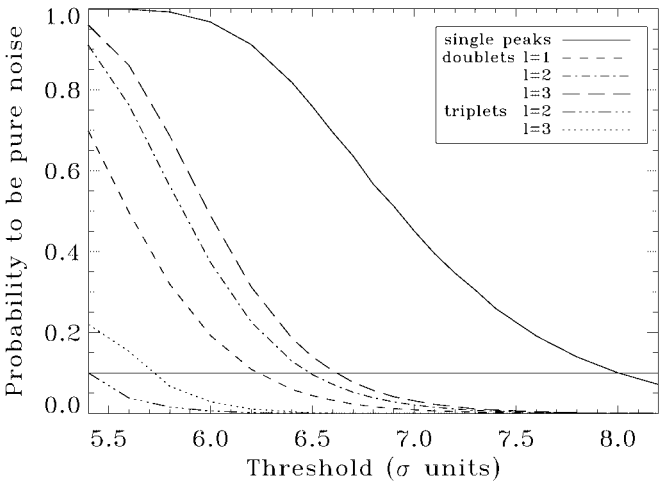

FIG. 3.—Computation of the threshold corresponding to a 90% confidence level for the MT with 4 sine tapers of the 1290 day long GOLF series. The threshold is given by the horizontal line crossing the different curves. Each type of multiplet has its own threshold.

the time period we are looking at (low and high activity). Second, we have checked on the periodogram, the AvCS, and the MT of real data that the statistical distribution we assumed for the solar noise was correct to a very good approximation. We made this between 150 and 1200 μHz, in regions where no high signal is expected. After the computation of the thresholds related to the confidence levels, we checked them by searching for multiplets and single peaks in intervals of 20 μHz between 150 and 1200 μHz (only in the intervals where neither *g*-modes nor *p*-modes were expected). The number of multiplets we detected for a given threshold was compatible with the expected one for the case of pure-noise series, confirming the validity of our thresholds.

5. RESULTS OBTAINED WITH A SERIES OF 1290 DAYS

We have shown that searching multiplets could be a good technique for reducing the amplitude of the detection threshold while keeping a high confidence level. In this section we apply the strategy described in § 2 to 1290 days of the GOLF data and we limit our analysis to a search of $l = 1$, 2, and 3 modes. We proceed in two steps. The first one is based on those single peaks that are above the threshold corresponding to more than 90% of not being pure noise. The second one is a search of multiplets that are not compatible with pure noise with the same confidence level.

On the region of interest (between 150 and 400 μHz), some acoustic modes are expected to be found ($l \leq 3$ with $n = 1$; see Bertello et al. 2000b; García et al. 2001a, 2001b). However, they are not explicitly searched for by the method adopted here. For example, we do not examine the band where a potential *p*-mode candidate $l = 1$, $n = 1$ has appeared at 284.666 or (and) 284.666 μHz with a very high confidence level in a previous work (Gabriel et al. 2002).

1. *Search for single peak*.—This search leads to very few detections, as was expected because of the amplitude of the *g*-mode. The automatic search leads to only two peaks at $\sim$218.95 and $\sim$262.13 μHz in the MT analysis. We find the same or some others if we play with the phase in the Fourier analysis, but we note that the amplitude of these peaks differs significantly between the periodogram and the MT analysis presented in Figures 4 and 5.

2. *Search for multiplets*.—As for the multiplet detection in Monte Carlo realizations, we search for multiplets on a power spectrum estimator by applying the "worst-case design." For instance, when looking for a doublet corresponding to an $l = 2$ mode, we enter as the separation parameter the frequency range 0.4–2.4 μHz, as if we were looking for the components $m = -2$ and $m = +2$. Neither a search of quadruplets—to detect $l = 3$ modes—nor a mixing of modes in the same region was computed in this analysis. So, the limitations of our multiplet detection algorithm are as follows:

a) When a peak is involved in a multiplet, we do not consider that it can be part of another multiplet. This gives a better result when computing the number of multiplets, but this could not be the case. For example, if four large-amplitude peaks are quite close (see for example Fig. 4), the algorithm will detect only one triplet using the first three peaks. Hence the results must be cautiously checked.

b) When looking for an $l = 3$ triplet and supposing that one component is missing, three possible combinations are considered depending on the searched components: three visible consecutive components or two consecutive ones and one distant.

Table 2 contains the results obtained with this automatic search. We list the single peaks, doublets, and triplets above a 90% confidence level for the periodogram and MT power spectrum estimators and compare them to the theoretical central frequencies of acoustic modes deduced from the seismic model of Turck-Chièze et al. (2001b). We detect slightly more multiplets than what we expect from pure-noise series. Some cases are at the limit of detection if we consider reexcitation in Fourier transform analysis. Consequently, the detected structures were separated in two types based on statistical considerations. The first class (hereafter, class A) corresponds to multiplets detected in the two power spectrum estimators. They correspond to Figures 4 and 5. Figures 6 and 7 illustrate the second class (hereafter, class B): clear detection in MT but presence of the structure below the 90% confidence level for the periodogram. We present five thresholds corresponding respectively to a 90% probability level for single peaks, doublets (for $l = 2$ and 3), and triplets (for $l = 2$ and 3). We observe several general behaviors:

1. In the class A patterns, we observe the same appearance of the structure in the different spectra, even if the confidence level can be extremely different.
2. The class A multiplets correspond to the candidates already discussed in Gabriel et al. (1998). We note that the amplitude of the multiplet components is too low to be detected in a search for individual peaks with a high confidence level.
3. The class B multiplets are different in each estimator.
4. Even though the GOLF instrument was designed to avoid any perturbation at the level of 1 mm s^{-1}, we cannot exclude that some instrumental noise or *SOHO* satellite noise exists at this level of amplitude, perturbing locally the candidate's statistical significance.

Some of the patterns may be *g*-mode candidates, but the identification task is not easy. We note that several modes of different degrees are expected to be separated by less than 5–10 μHz, including modes $l = 4$, 5, which may interfere with the modes we are looking for. This is the reason why their theoretical positions are mentioned on the figures. Moreover, some of the components may be absent, and since we have not yet detected a *g*-mode excited by convection turbulence, we

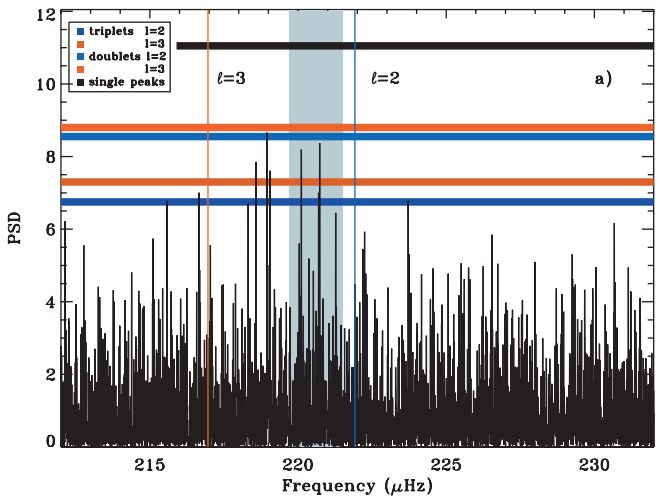

FIG. 4*a*

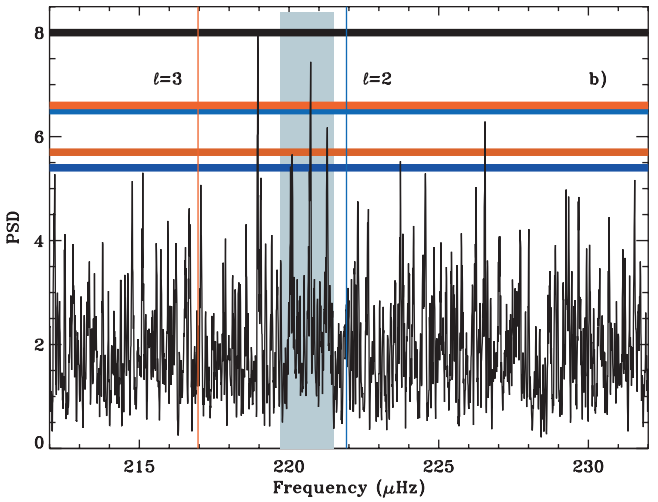

FIG. 4*b*

FIG. 4.—Example of the class A pattern. (*a*) Periodograms of 1290 days with zero-padding by a factor of 3, centered on the predicted $l = 2$, $n = -3$. (*b*) MT estimate. The 90% confidence levels of not being noise are shown by the black line for single peaks, the blue (light or dark) lines for respectively doublets and triplets corresponding to $l = 2$, and the red (light or dark) lines for respectively doublets and triplets corresponding to $l = 3$. The gray area on the plots corresponds to the region where a structure has been identified in one or several methods.

do not yet really know how it will look. This is why we have decided to use longer series and see the evolution of the patterns.

6. EVOLUTION WITH TIME OF THE DETECTED PATTERNS

We have done a second and third analysis after 1768 and 2034, days illustrated respectively by Figures 8 and 9, using the MT analysis, which has been established as the most reliable for modes of mixed character. In these two new series the previously detected triplets are no longer detected at a 90% confidence level, even though still present. There appear two new triplets at 156.24, 156.99, and 157.90 μHz (class B) and at 178.57, 179.08, and 179.51 μHz (typical class A). The last one is present in the two longest series (1768 and 2034 days) and in the periodogram and MT estimators. Such structure was also present in the shorter series with a low significance level. The pattern around 340 μHz has disappeared (Figs. 6, 8, and 9). The reasons for this time evolution may be of different origin:

1. The detected patterns are in fact due to noise. This cannot be excluded since we work at the detection limits, with a very small number of frequency intervals.
2. The increase of activity could prevent us from detecting structures near the maximum of solar activity. At the region of interest, 150–400 μHz, the level of solar noise increases by up to a factor of 2. Moreover, a detailed study of acoustic modes for GOLF and VIRGO along the same period shows that the width of the modes increases with activity and the amplitudes decrease (Jiménez-Reyes et al. 2003). Thus, the data added during this period have a lower signal-to-noise ratio. It seems to be clear that the high activity is certainly the worst period for

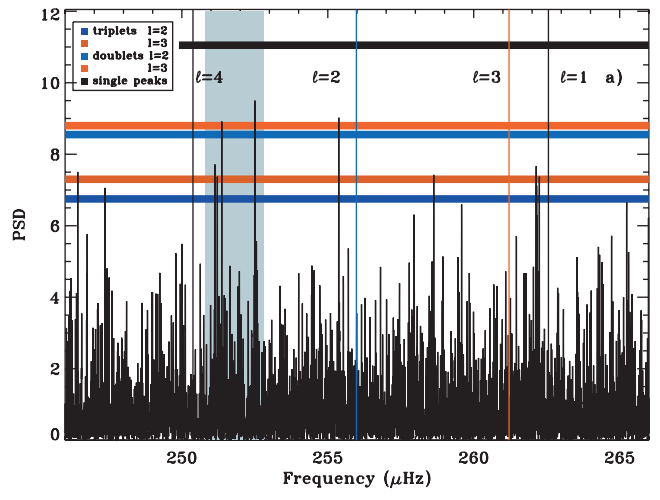

FIG. 5*a*

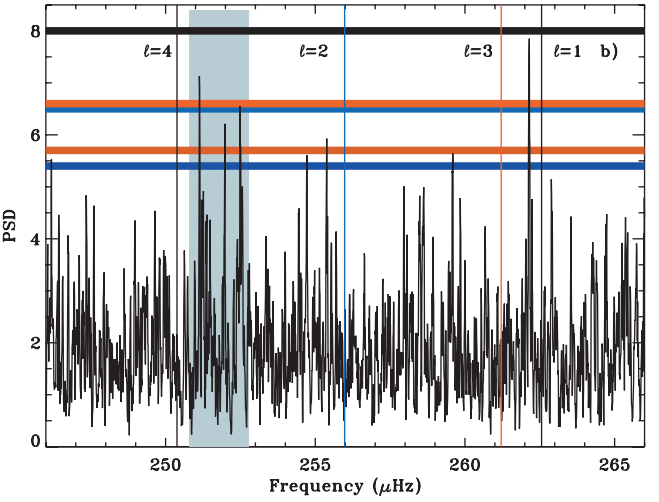

FIG. 5*b*

FIG. 5.—Example of the class A pattern. (*a*) Periodogram of 1290 days with zero-padding centered on the predicted $l = 2$, $n = -2$. (*b*) MT estimate. Same representation as in Fig. 4.

TABLE 2

THE g-MODE PATTERNS WITH MORE THAN 90% CONFIDENCE LEVEL OF NOT BEING NOISE COMPARED WITH THE THEORETICAL CENTRAL VALUE FOR 1290 DAYS OF GOLF OBSERVATIONS

Order	Seismic Model (μHz)	Periodogram (μHz)	Multitaper (μHz)
		$l = 1$	
$n = -3$	153.25	...	...
$n = -2$	191.55	196.94/198.01	...
$n = -1$	262.73	...	262.15
		$l = 2$	
$n = -6$	151.26	144.63/145.62/146.60	...
$n = -5$	170.46	...	...
$n = -4$	194.06	...	193.86/195.25
$n = -3$	222.02	218.95/220.10/220.70	218.95/220.10/221.28
$n = -2$	256.09	251.37/252.5	251.14/252.48
$n = -1$	296.38	...	...
		$l = 3$	
$n = -9$	148.33	146.79/149.99	...
$n = -8$	161.72	...	...
$n = -7$	177.46	...	171.56/172.26/173.56
$n = -6$	195.93	...	193.86/195.25
$n = -5$	217.07	218.95/220.11/220.73	218.96/220.72
$n = -4$	238.35	...	...
$n = -3$	261.31	251.37/252.5	262.15
$n = -2$	296.50	...	...
$n = -1$	340.07	...	337.56/338.01/338.94

looking for g-modes, and this is why we have decided to wait until the next solar minimum for continuing this analysis.

3. After the *SOHO* vacation, the observation is done on the right part (red wing) of the sodium doublet at higher altitudes in the solar atmosphere and with a different sensitivity over the solar disk. Considering the evanescent character of the gravity modes, the amplitude of these modes measured at a higher altitude must be weaker, and it appeared to be better to switch back to the initial blue wing GOLF configuration. This was done on 2002 November 18. So, we will still have 4 years of observation with an increased signal-to-noise ratio.

7. DISCUSSION

The present analysis has reduced the amplitude of the velocity level where gravity-mode candidates may be found to 2 mm s^{-1}. Successive analyses have probably eliminated several noise peaks that do not persistently appear along the whole analysis.

However, in the longest series, the evolution of the structures called class A is interesting to analyze. For example, the pattern located around 220 μHz has a persistent character with many organized peaks. What is the probability of finding such signal? To answer this question we have looked for quintuplets and even sextuplets with a more than 90% confidence level, without making any assumptions on the degree of the mode.

In fact we have found three (slightly more than expected) quintuplets from 218.31 to 220.72 μHz, 236.05 to 238.53 μHz, and 241.64 to 243.61 μHz and two sextuplets from 218.31 to 221.27 μHz and 260.77 to 264.26 μHz. Of course their amplitudes are very small and also very near to the noise level. Figure 10 illustrates the two most interesting patterns. Case 1 shows peaks at 218.31, 218.95, 219.59, 220.12, 220.72, and 221.26 μHz; for case 2, the values are 260.77, 261.51, 262.14, 262.86, 263.54, and 264.26 μHz. The corresponding velocities are about $\sim 2 \pm 0.9$ mm s^{-1} on an MT estimator, very near to the limit of the GOLF instrument. In both of them, the peaks are rather well spaced. This is not the case for the other patterns, which are probably perturbed by larger noise contributions. We know from a theoretical point of view that modes of up to $l = 6$ have energy inertia (PBM00) similar to that of low-degree modes (we note the theoretical positions on the figures), so it is probably interesting to optimize some masks to amplify their visibility. Wachter et al. (2002) worked on this direction and showed some results for $l = 1$ and 2, noting that some components of $l = 2$ may be bigger than some others of $l = 1$. Nevertheless, in a disk-integrated instrument such as GOLF, the sensitivity to higher degrees is slightly reduced, so the potential detection of quintuplets does not seem to be naturally explained by invoking $l = 4$ or 5 modes, even if an interference between modes may contribute to some specific peaks. It would remain nevertheless troublesome to label a pattern around 251.8 μHz, if this pattern exists, without invoking an $l = 4$, $n = -5$ mode.

What could be the consequences if the structures detected in this paper end up being low-degree gravity modes? Let us comment on case 1:

1. The peaks could correspond to adjacent modes, typically $l = 2$, $n = -3$ and $l = 3$, $n = -5$, and the observed splitting of 600 nHz between components could suggest a synodic splitting of 300 nHz, which corresponds to a lower rotation in the very central part of the Sun.

2. The peaks could come from the same mode, typically $l = 2$, $n = -3$ or $l = 3$, $n = -5$. If we observe five components, that means that all the components are present. So, the

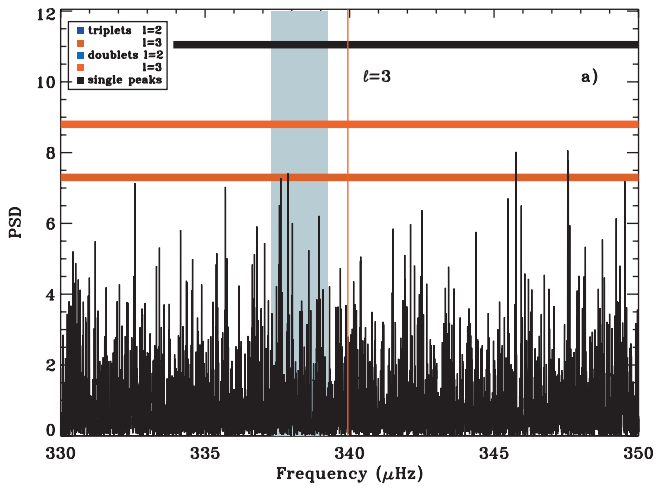

FIG. 6*a*

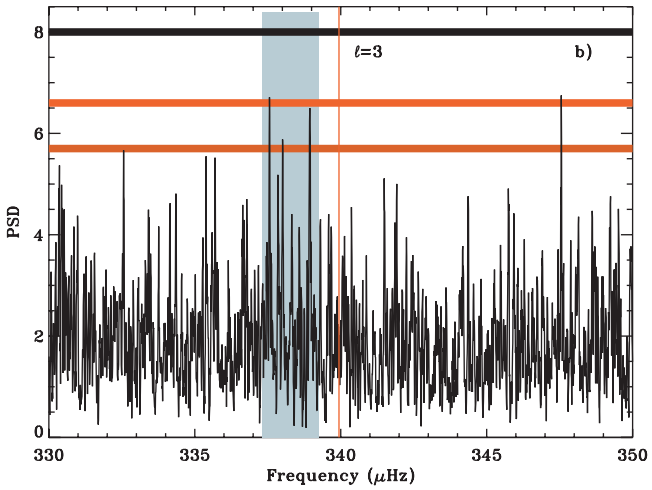

FIG. 6*b*

FIG. 6.—Example of the class B pattern. (*a*) Periodogram of 1290 days with zero-padding, centered on the predicted $l = 3$, $n = -1$. (*b*) MT estimate. Same representation as in Fig. 4, but restricted to the $l = 3$ cases.

rotation axis in the core is different from that in the rest of the Sun, and the synodic splitting of 600 μHz means that the Sun rotates quicker in its very central region than in the rest of the radiative zone. Such a situation has been suggested as possible by Gough (1999).

3. The interpretation of this pattern could be complicated by the presence of an $l = 5$ mode in the neighborhood.

Case 2, corresponding to the pattern around 262 μHz, could be interpreted in the same way considering $l = 1$, $n = -1$ and $l = 3$, $n = -3$, which are very near; the splittings would be slightly larger, and the interpretation of this case is also complicated by the presence of an $l = 4$ mode in the neighborhood.

With 2034 days of observations, we reach an excellent resolution ($\Delta\nu = 5.69$ nHz). We notice the existence of fine structure in the peaks, quite visible in Figure 10. If this is not due to pure noise or interference between modes, it is not excluded that the detected components have different peaks, spaced by about ~100 nHz. This could be some effect coming from a central magnetic field with an axis different from the rotational one, as was suggested by Goode & Thompson (1992), but probably we go too far in analyzing the present data. It is clear that such patterns will be extremely exciting to follow with time during the next solar minimum.

8. CONCLUDING REMARKS

We have proposed a new strategy based on the search for multiplets that allows us to look for patterns down to 2 ± 1 mm s^{-1} after ~2000 days of observation. This limit is 30 to 40 times below what had been analyzed on the ground before *SOHO*. These detections are at the sensitivity limit of GOLF and not far from the expected theoretical visibility of the *g*-modes.

Some interesting patterns (four) have been identified with a 90% confidence level of not being pure noise in series of 1290

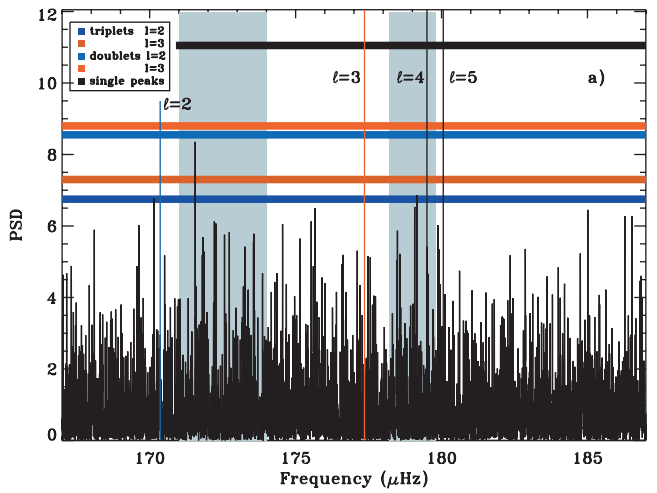

FIG. 7*a*

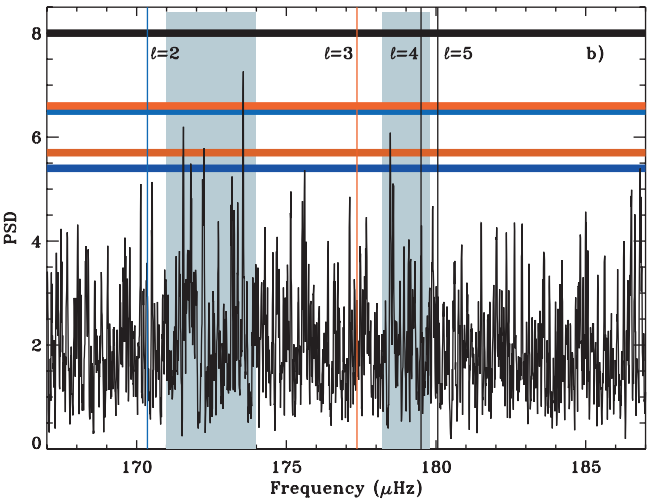

FIG. 7*b*

FIG. 7.—Example of the class B pattern. (*a*) Periodograms of 1290 days with zero-padding, centered on the predicted $l = 3$, $n = -7$. (*b*) MT estimate. Same representation as in Fig. 4.

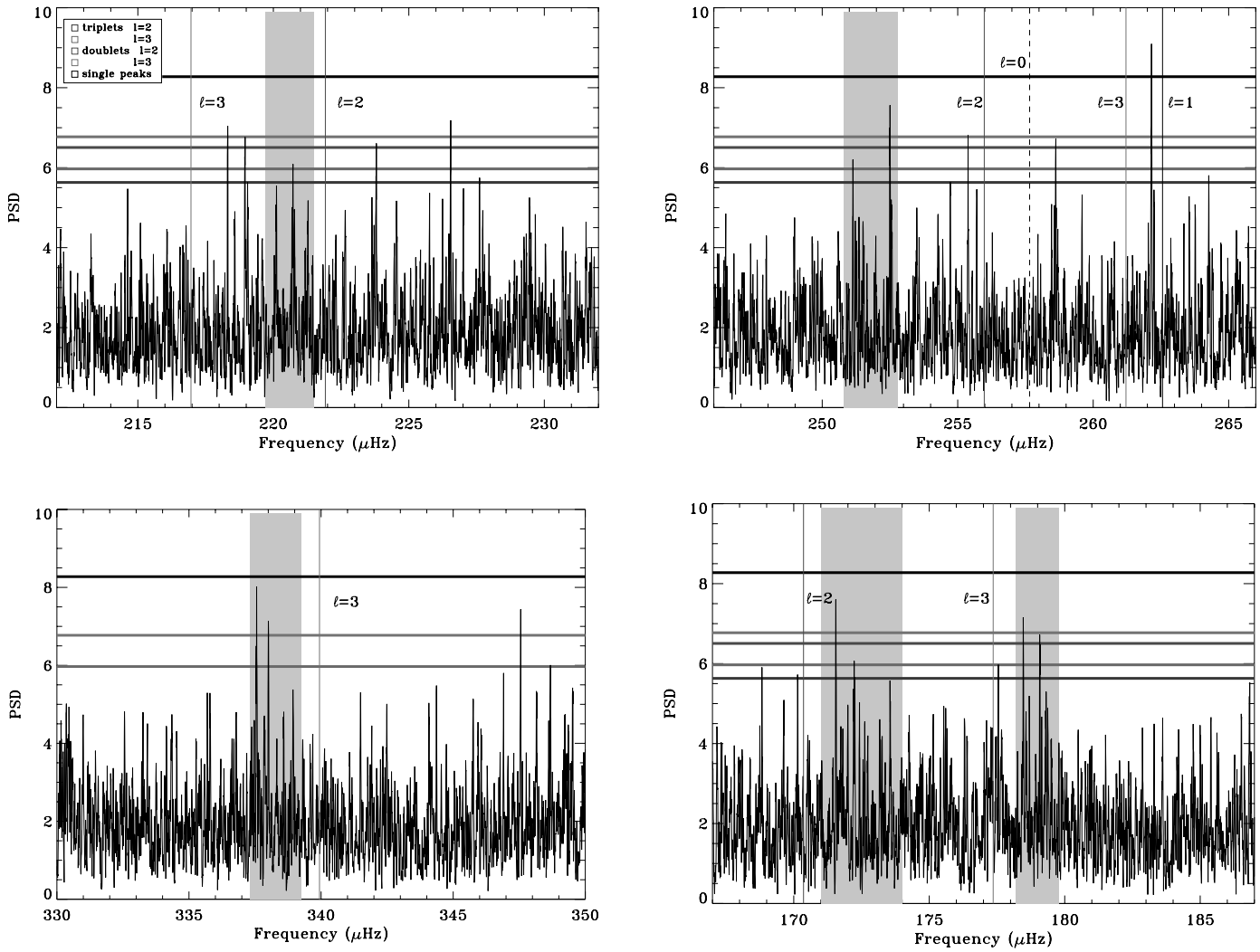

FIG. 8.—MTs of 1768 days for the four previous cases. No structures have been detected except a triplet near 180 μHz, but some interesting peaks are still present (see text). [*See the electronic edition of the Journal for a color version of this figure.*]

days. Two of them have been detected by at least two different power spectrum estimators.

We have followed the evolution with time of the corresponding 20 μHz interval around values where g-modes were expected (from 150 to 400 μHz), during 5 years in the GOLF data, with the goal of eliminating the less convincing patterns or progressing on potential identifications. Some of these candidates have effectively disappeared with the longer series (for example, the case at 340 μHz), maybe because of their noisy nature, while the shape of some others has evolved (the case around 220 μHz, for example) without increasing their confidence level. Other new patterns have also appeared interesting to pursue. This fact is not totally discouraging since several factors have altered the detection condition after the *SOHO* vacation: the place in the line where we detect the phenomenon, the activity of the Sun, which leads to a degradation of the signal-to-noise ratio, and the mixed character of the searched modes, which leads to probable re-excitation of the modes, giving resolved widths.

Today we cannot arrive at a firmly established conclusion, but we cannot exclude the possible detection of several components of g-mode candidates. Two extremely interesting cases have justified complementary studies and several possible physical interpretations. They can be summarized by the following questions: Are the GOLF data telling us that the Sun rotates differently in the very central region? Is there some central or external magnetic field effect visible in the appearance of the gravity-component candidates? Are we able to see some $l = 4$ gravity components with a disk-integrated instrument?

The present analysis may suggest that some g-mode–like structures, located at the frontier of the acoustic modes, in the mixed-mode region, are not simple and thin structure, as suggested by long-lifetime g-modes. The situation is sufficiently puzzling for us to remain extremely cautious and to encourage activities on the visibility of the modes. Since GOLF is now returning to the blue part of the line, we are confident of making conclusions on the existence of gravity modes in the observations before the end of the life of *SOHO* in 2007, adding better ratios of signal (if any) to noise during this period of decreased activity. In this study we have looked only for g-modes, but we need to mention that the radial mode $n = 1$ is located in the second panel of Figures 8 and 9 near 258 mHz. A peak is effectively present with less than 90% confidence level in its neighborhood. It will be interesting to follow this in time. Another pattern at 284.666 or 286.781 μHz has been mentioned by Gabriel et al. (2002) in the vicinity of an expected $l = 1$, $n = 1$, so there are several reasons

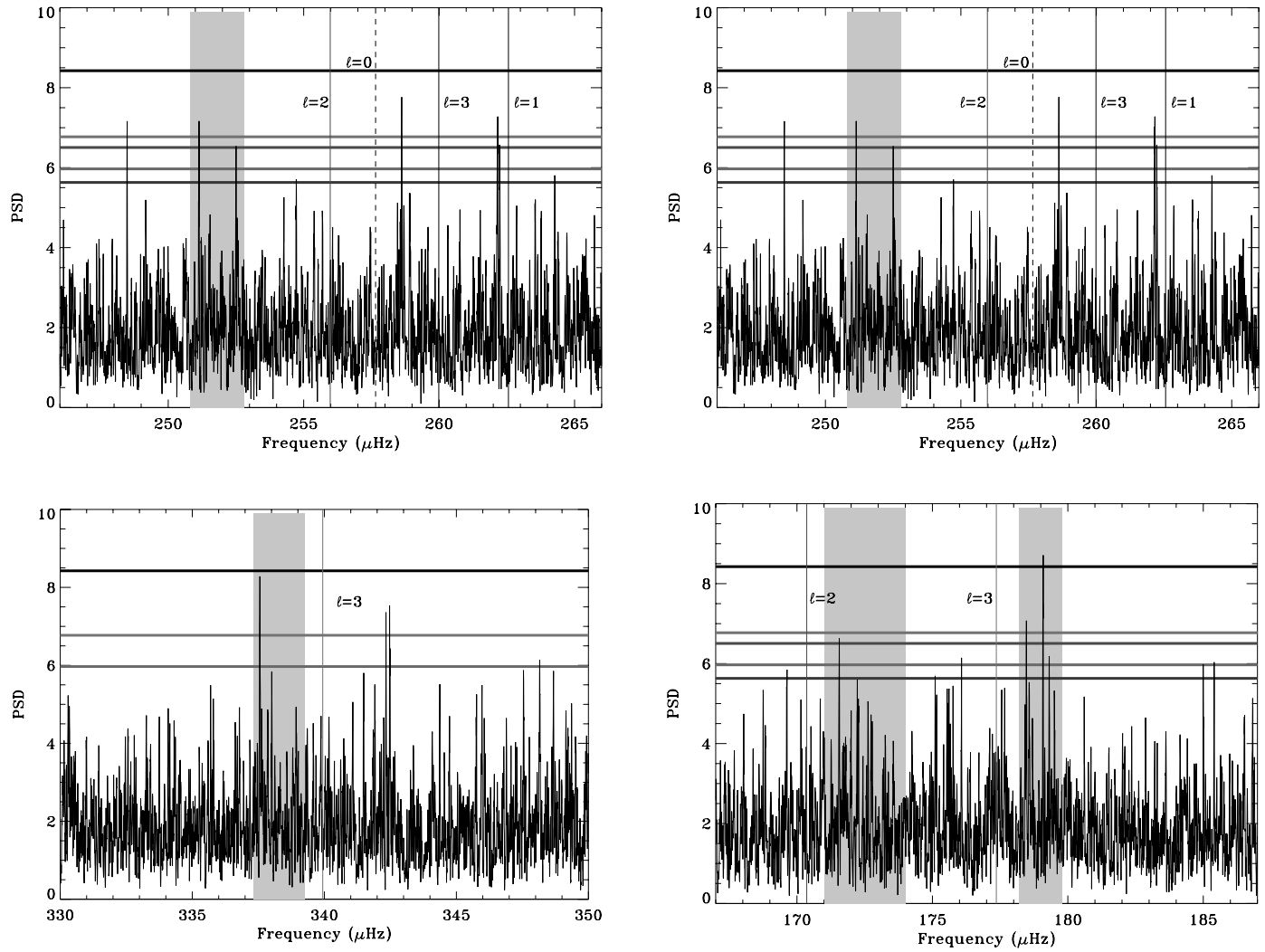

FIG. 9.—MTs of 2034 days for the four previous cases. No structures have been detected except a triplet near 180 μHz, but some interesting peaks continue to be present and some others disappear (see text). [*See the electronic edition of the Journal for a color version of this figure.*]

to await further analysis with real hope of progress in this field.

A combination of GOLF, MDI, and VIRGO data has not yet really helped to draw any conclusions, since a common analysis depends on the noise level of the best instrument, but efforts will be pursued in this direction during observations of the quiet Sun. A next generation of instrument, attacking directly the problem of solar noise, is under construction. The idea is to get simultaneous measurements of the velocity at different constant heights of the atmosphere to reduce the

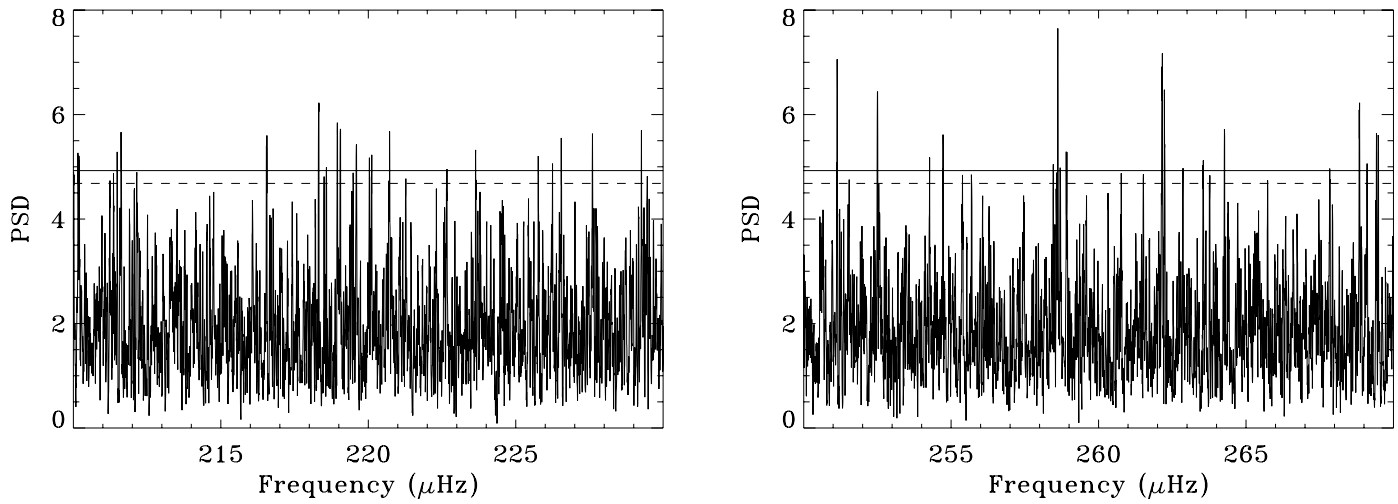

FIG. 10.—Detection of the most interesting quintuplets (*continuous line*) or sextuplets (*dashed line*) with more than 90% probability of containing signal

effects of the intrinsic variability of the line (Turck-Chièze et al. 2001c). A prototype, built by an international consortium, will be available in about a year, with the aim of building a space version in the next decade.

The GOLF experiment is based on a consortium of institutes involving a large number of scientists and engineers, belonging to the IAS (France), the CEA (France), the IAC (Spain), and the observatories of Bordeaux and Nice (France). *SOHO* is a mission of international cooperation between ESA and NASA. The authors would like to thank the CNES agency for its strong support all these years, C. Renaud and J. Charra for their daily work surveying the GOLF experiment, and T. Foglizzo for many enlightening discussions related to this work.

APPENDIX A

THE PERIODOGRAM ESTIMATOR

This is the squared Fourier transform of the full length—1290, 1768, and 2034 days—velocity-averaged time series $[(V_{\rm PM1} + V_{\rm PM2})/2]$ with a sampling time $\delta t = 80$ s. It is well known that this method has four limitations: (1) There is a power leakage for every peak, due to the rectangular observational window. (2) The variance of the estimate is large in comparison with averaging methods. (3) A high-amplitude peak whose frequency lies between two bins of the periodogram will appear on this estimator with a reduced amplitude. In the worst case, the observed amplitude is reduced by 40%, compared with the real one. To reduce the effect of this problem, we use zero-padding. We add N zeros at the end of the time series (3 times the length of the data series) and compute the periodogram of this new time series. Thus, the resolution on the periodogram is increased but the bins on the new power spectrum are no longer independent. The last point discussed in § 3.1 is that (4) the amplitude of a peak can be reduced by a phase shift. To deal with this problem of the possible re-excitation of a candidate, we have examined different estimates with a 0° and a 180° phase shift (we have chosen the shift arbitrarily) after the *SOHO* vacation period, but present only the first one in the present paper.

APPENDIX B

THE AVERAGED–CROSS SPECTRUM ESTIMATOR

This is the average of several cross spectra computed between the two velocity channels PM1 and PM2. The two complete time series are divided into K subseries, and estimates of their PSDs are computed:

$$\mathrm{PSD}(\nu) = \frac{\sum_{k=0}^{N-1} \left| \mathcal{F}(V_{\mathrm{PM1},k})\, \mathcal{F}(V_{\mathrm{PM2},k})^* \right|}{N}, \tag{B1}$$

where $\mathcal{F}(V_{\mathrm{PM}i,k})$ is the Fourier transform of the kth subseries for the velocity residual of the ith photomultiplier. For the 1290 day long series, we have used subseries of 129 days, which is a good trade-off between the frequency resolution and the number of independent subseries to average. One subseries of 129 days was rejected because of its low duty cycle. This approach reduces the variance in the estimates and the incoherent noise between the two velocity signals but deteriorates the frequency resolution to $\Delta\nu = 89.7$ nHz. This estimator was especially useful at the beginning of the g-mode search for following the multiplet patterns in each individual subset and in the average one, and it has led to the presentation of two candidates by Gabriel et al. (1998). With very long series, this method appears less promising than the other ones, because of its lower individual resolution. As we have already said, we have decided to remove from this paper a detailed analysis based on this technique. However, the conclusions are not substantially modified when they are taken into account.

APPENDIX C

THE MULTITAPER SPECTRUM ESTIMATOR

This method (Fodor & Stark 1998; Komm et al. 1998) reduces the power leakage due to the rectangular observational window and is known to give a better PSD estimate than the periodogram (Percival & Walden 1993). Moreover, the effect of a phase shift in the resonances is minimized to less than 3% of the total power. No special treatment of data gaps has been made, despite the *SOHO* summer vacation, because of the high duty cycle of GOLF. The time series are multiplied by K (here 4) windows (the so-called tapers), and the average of the corresponding periodograms is computed. Therefore, an MT spectrum is the average of K asymptotically independent periodograms:

$$\mathrm{PSD}(\nu) = \frac{1}{K}\sum_{k=0}^{K-1} \mathrm{PSD}_k(\nu), \text{ with } \mathrm{PSD}_k(\nu) = \delta t \left| \sum_{t=0}^{N-1} h_{t,k} V_i \exp\left(-i2\pi f t \delta t\right) \right|^2, \tag{C1}$$

where δt is the sampling interval, $h_{t,k}$ are the tapers, and V_i are our time series. The chosen tapers are sine functions. Since it is an average, the variance of the MT estimate is reduced by a factor $1/K$ compared to the variance of the periodogram, but the central lobe of the peaks is broadened and its amplitude is slightly reduced. The choice of four tapers is a good trade-off between protection against power leakage and protection against "peak broadening."

APPENDIX D

THE RANDOM-LAG SINGULAR CROSS SPECTRUM ANALYSIS

This new approach was recently developed by Varadi et al. (2000) and was originally designed to search for coherent oscillations in short and noisy time series in geophysics (e.g., Dettinger et al. 1995). The RLSCSA searches for oscillations in noise by the singular value decomposition (Golub & Van Loan 1996) of cross-correlation matrices into a diagonal form that provides the corresponding eigenvalues and eigenvectors.

In order to efficiently apply the RLSCSA, the time series have to go through a preliminary data reduction. This process includes the following steps: First, in order to reduce the length of the time series and since we are interested in modes with frequencies below 1.5 mHz, we subsampled the time series to 300 s. This task is accomplished by applying a low-pass digital filter to the original time series with a cutoff frequency that is the Nyquist frequency corresponding to the final sampling. The application of the filter before the subsampling is necessary to assure that signal distortion due to aliasing is negligible. Second, a high-pass filter with cutoff at 0.1 mHz is used to eliminate spectral leakage from the very low frequency range.

The capability of the RLSCSA for producing clean mode profiles was first demonstrated by Bertello et al. (2000b) for a 804 day long sequence of data from GOLF and MDI. This method has been used to detect low-frequency acoustic modes.

REFERENCES

Andersen, B. N. 1994, Sol. Phys., 152, 247
———. 1996, A&A, 312, 610
Appourchaux, T., et al. 2000, ApJ, 538, 401
Basu, S., Turck-Chièze, S., & Berthomieu, G. 2000, ApJ, 535, 1078
Bertello L., Henney C. J., Ulrich R. K., Kosovichev A. G., Roca Cortés T., Thiery S., Boumier, P., & Turck-Chièze, S. 2000a, ApJ, 535, 1066
Bertello, L., Varadi, F., Ulrich, R. K., Henney, C. J., Kosovichev, A. G., García, R. A., & Turck-Chièze, S. 2000b, ApJ, 537, L143
Brun, A. S., Turck-Chièze, S., & Morel, P. 1998, ApJ, 506, 913
Brun, A. S., Turck-Chièze, S., & Zahn, J. P. 1999, ApJ, 525, 1032
Corbard, T., Berthomieu, G., Provost, J., & Morel, P. 1998, A&A, 330, 1149
Corbard, T., Blanc-Féraud, L., Berthomieu, G., & Provost, J. 1999, A&A, 344, 696
Couvidat, S. 2003, Ph.D. thesis, Univ. Paris VII
Couvidat, S., García, R. A., Turck-Chièze, S., Corbard, T., Henney, C. J., & Jiménez-Reyes, S. 2003a, ApJ, 597, L77
Couvidat, S., Turck-Chièze, S., & Kosovichev, A. G. 2003b, ApJ, 599, 1434
Delache, P., & Scherrer, P. H. 1983, Nature, 306, 651
Demarque, P., & Robinson, F. J. 2003, Ap&SS, 284, 193
Denison, D. G. T., & Walden, A. T. 1999, ApJ, 514, 972
Dettinger, M. D., Ghil, M., Strong, C. M., Weibel, W., & Yiou, P. 1995, Eos, 76, 12
Dzitko, H. 1995, Ph.D. thesis, Univ. Paris XI
Elliott, J. R., & Gough, D. O. 1999, ApJ, 516, 475
Elliott, J. R., & Kosovichev, A. G. 1998, ApJ, 500, L199
Fröhlich, C., & Delache, P. 1984, Mem. Soc. Astron. Italiana, 55, 99
Fröhlich, C., et al. 1995, Sol. Phys., 162, 101
Fodor, I. K., & Stark, P. B. 1998, in Structure and Dynamics of the Interior of the Sun and Sun-like Stars, ed. S. Korzennik & A. Wilson (ESA SP-418; Noordwijk: ESA), 171
Gabriel, A. H., et al. 1995, Sol. Phys., 162, 61
———. 1997, Sol. Phys., 175, 207
———. 1998, in Structure and Dynamics of the Interior of the Sun and Sun-like Stars, ed. S. Korzennik & A. Wilson (ESA SP-418; Noordwijk: ESA), 61
———. 2002, A&A, 390, 1119
García, R. A., Turck-Chièze, S., & Boumier, P. 2003, A&A, submitted
García, R. A., et al. 2001a, Sol. Phys., 200, 361
———. 2001b, in Helio- and Asteroseismology at the Dawn of the Millennium, ed. A. Wilson (ESA SP-464; Noordwijk: ESA), 473
Golub, G. H., & Van Loan, C. F. 1996, Matrix Computations (Baltimore: Johns Hopkins Univ. Press)
Goode, P. R., & Thompson, M. J. 1992, ApJ, 395, 307
Gough, D. O. 1999, Nucl. Phys. B (Proc. Suppl.), 77, 81
Harvey, J. 1985, Future Missions in Solar, Heliospheric, and Space Plasma Physics, ed. E. Rolfe & B. Battrick (ESA SP-235; Noordwijk: ESA), 199
Jiménez-Reyes, S., García, R. A., Jiménez, A., & Chaplin, W. J. 2003, ApJ, 595, 446
Komm, R. W., Anderson, E., Hill, F., Howe, R., Fodor, I., & Stark, P. 1998, in Structure and Dynamics of the Interior of the Sun and Sun-like Stars, ed. S. Korzennik & A. Wilson (ESA SP-418; Noordwijk: ESA), 257
Kosovichev, A. G., & Gavryuseva, E. A. 1995, in ASP Conf. Ser. 76, GONG '94: Helio and Astero-Seismology, ed. R. K. Ulrich, E. J. Rhodes, Jr., & W. Däppen (San Francisco: ASP), 180
Kosovichev, A. G., et al. 1997, Sol. Phys., 170, 43
Kumar, P., Quataert, E. J., & Bahcall, J. N. 1996, ApJ, 458, L83
Kumar, P., Quataert, E. J., & Eliot, J. 1997, ApJ, 475, L143
Kumar, P., Talon, S., & Zahn, J.-P. 1999, ApJ, 520, 859
Lopes, I., & Gough, D. 2001, MNRAS, 322, 473
Lopes, I., & Turck-Chièze, S. 1994, A&A, 290, 845
Maeder, A., & Meynet, G. 2000, A&A, 361, 159
Martín Mateos, I., & Pallé, P. L. 1999, Sol. Phys., 189, 241
Nigam, R., & Kosovichev, A. G. 1999, ApJ, 510, L149
Pallé, P. L., Roca Cortés, T., Gelly, B., Pérez-Hernández, F., & the GOLF Team. 1998, in Structure and Dynamics of the Interior of the Sun and Sun-like Stars, ed. S. Korzennik & A. Wilson (ESA SP-418; Noordwijk: ESA), 279
Percival, D. B., & Walden, A. T. 1993, Spectral Analysis for Physical Applications: Multitaper and Conventional Univariate Techniques (Cambridge: Cambridge Univ. Press)
Provost, J., Berthomieu, G., & Morel, P. 2000, A&A, 353, 775 (PBM00)
Scherrer, P. H., et al. 1995, Sol. Phys., 162, 129
Takata, M., & Shibahashi, H. 1998, ApJ, 504, 1035
Thiery, S., Boumier, P., Gabriel, A. H., Henney, C. J., & the GOLF Team. 2001, in Helio- and Asteroseismology at the Dawn of the Millennium, ed. A. Wilson (ESA SP-464; Noordwijk: ESA), 681
Thiery, S., et al. 2000, A&A, 355, 743
Thomson, D. J., Maclennan, C. G., & Lanzerotti, L. J. 1995, Nature, 376, 139
Toutain, T., et al. 1997, Sol. Phys., 175, 311
Turck-Chièze, S., Brun, A. S., Chièze, J. P., & García, R. A. 1998a, in Structure and Dynamics of the Interior of the Sun and Sun-like Stars, ed. S. Korzennik & A. Wilson (ESA SP-418; Noordwijk: ESA), 549
Turck-Chièze, S., Nghiem, P., Couvidat, S., & Turcotte, S. 2001a, Sol. Phys., 200, 323
Turck-Chièze, S., et al. 1997, Sol. Phys., 175, 247
———. 1998b, in Structure and Dynamics of the Interior of the Sun and Sun-like Stars, ed. S. Korzennik & A. Wilson (ESA SP-418; Noordwijk: ESA), 555
———. 2001b, ApJ, 555, L69
———. 2001c, in Helio and Asteroseismology at the Dawn of the Millennium, ed. A. Wilson (ESA SP-464; Noordwijk: ESA), 331
Ulrich, R. K., Boumier, P., Robillot, J. M., & García, R. A. 2000a, A&A, 364, 816
Ulrich, R. K., et al. 2000b, A&A, 364, 799
van der Raay, H. B. 1988, in Seismology of the Sun and Sun-like Stars (ESA SP-286; Noordwijk: ESA), 339
Varadi, F., Ulrich, R. K., Bertello, L., & Henney, C. J. 2000, ApJ, 528, L53
Vorontsov, S. V., Baturin, V. A., & Pamyatnykh, A. A. 1991, Nature, 349, 49
Wachter, R., Schou, J., Kosovichev, A. G., & Scherrer, P. H. 2002, in From Solar Min to Max: Half a Solar Cycle with *SOHO*, ed. A. Wilson (ESA SP-508; Noordwijk: ESA), 115
Zahn, J. P., Talon, S., & Matias, J. 1997, A&A, 322, 320